

General Disclaimer

One or more of the Following Statements may affect this Document

- This document has been reproduced from the best copy furnished by the organizational source. It is being released in the interest of making available as much information as possible.
- This document may contain data, which exceeds the sheet parameters. It was furnished in this condition by the organizational source and is the best copy available.
- This document may contain tone-on-tone or color graphs, charts and/or pictures, which have been reproduced in black and white.
- This document is paginated as submitted by the original source.
- Portions of this document are not fully legible due to the historical nature of some of the material. However, it is the best reproduction available from the original submission.

NAG 5-185

(NASA-CR-170117) WARM WATER MASS FORMATION
(Woods Hole Oceanographic Institution) 58 p
HC A04/MF A01 CSCI 08J

N83-21731

Unclas
G3/48 03173

Warm Water Mass Formation

G.T. Csanady

Woods Hole Oceanographic Institution
Woods Hole, Massachusetts 02543



Woods Hole Oceanographic Institution Contribution Number

Abstract

Poleward heat transport by the ocean implies warm water mass formation, i.e. the retention by the tropical and subtropical ocean of some of its net radiant heat gain. Under what conditions net heat retention becomes comparable to latent heat transfer to the atmosphere depends on the relative efficiency of transfer processes across the air-sea interface, the top of the atmospheric mixed layer, and the floor of the oceanic mixed layer. A thermodynamic model of the interacting atmospheric and oceanic mixed layers, with the top of the atmospheric layer taken to be at cloud base, shows that net oceanic heat retention is significant under the following circumstances.

(1) Seasonal heat storage, amplitude of order 100 W m^{-2} . This is a fairly straightforward consequence of the large heat capacity of the oceanic mixed layer and leads the seasonal forcing by about a month.

(2) Massive upwelling (vertical velocity of order 10^{-5} m s^{-1}), mostly along equatorial cool tongues, with net heat retention of order 100 W m^{-2} . The upwelling cooler water is heated and transported away mainly by the divergence of surface layer flow (less by the increasing temperature in the direction of the flow).

(3) Cold water advection, mostly within the subtropical gyres, net heat retention of order 30 W m^{-2} . The latitudinal variation of radiant heating, and generally equatorward surface flow in the northern portions of subtropical gyres leads to a moderate rate of warming of the water column as it moves along, i.e. to net heat retention of the above order.

A comparison of model results with observation shows that, over the subtropical gyres, observed temperature and humidity relationships can only be

simulated realistically if cold water advection is taken into account. In addition, it is necessary to suppose that the transfer coefficient at the top of the atmospheric mixed layer (at cloud base) is about as large as at the sea surface, while the transfer coefficient at the oceanic mixed layer floor is negligible, except in regions of massive upwelling. The general dominance of latent heat transfer arises from the large value of a nondimensional latent heat coefficient (a material property) and from the rapid drop of saturation specific humidity with height in the atmosphere.

Introduction

It is now widely accepted that the ocean transports heat poleward at a rate that at certain latitudes is of the order of 1 petawatt (10^{15} W), see e.g. Hastenrath (1982). The global process is illustrated schematically in Fig. 1: in order to balance the net heat loss of the polar ocean, water at an average temperature $T_p > T_E$ is transferred poleward (either by "mean" flow or by "eddies"), at the rate $M[\text{kg s}^{-1}]$. From the available temperature and salinity differences and heat and freshwater transports it may be shown (Stommel and Csanady, 1980) that M/ρ is of order $10^8 \text{ m}^3 \text{ s}^{-1}$. A similar result is obtained by direct oceanic heat transport and heat budget calculations (Bryden and Hall, 1980; Wyrki, 1981).

At high latitudes, therefore, water is cooled at the aggregate rate of $M \text{ kg s}^{-1}$, a process that results in "water mass formation", i.e. a major change of the temperature and salinity characteristics of the water masses involved. The mechanism of this process is fairly well understood: it involves vigorous penetrative convection, vertical mixing, frequently, but not always, a descent of the newly formed mixture to some subsurface level and its eventual escape equatorward.

A counter-process of warm water mass formation necessarily exists in the tropical ocean in order to regenerate water masses of higher temperature and salinity than enter from higher latitudes. This process is less well understood. In contrast to surface cooling, heating increases stability and tends to retard vertical exchange. Thus except where the cooled water remains at the surface and flows equatorward, some other mechanism, independent of the surface heating process (and in fact counteracting the latter's stabilizing influence) must be present to expose deeper layers to the atmosphere. Only

then is it possible to fuel the warm water mass formation process at the required rate and allow the global cycle sketched in Fig. 1 to be completed.

Both atmospheric and oceanic heat budgets show that the principal mechanism supplying cooler water to the surface layer is equatorial upwelling (Hastenrath, 1980, 1982; Wyrski, 1981). Of lesser importance is coastal upwelling. Cold water advection in the surface layer from high to low latitudes, not involving descent associated with cooling in the first place, is also significant, but contributes much less on a global scale than equatorial upwelling.

Thus the main features of the global oceanic heat transport cycle are known. It is not clear at all, however, what the controls of this cycle are. What determines the mass transfer rate M , the temperatures T_p and T_E , and therefore the net heat transport $Q_H = C_w M(T_p - T_E)$? Why does the ocean not carry an even greater fraction of the total atmospheric-oceanic poleward heat transport than it does, when solar radiation is absorbed in the first instance in the top layer of the ocean, and when the heat capacity of the ocean is so much greater than that of the atmosphere? The proximate cause of the relatively large atmospheric heat transport is evaporation from extensive areas of the tropical and subtropical ocean, and the subsequent release of latent heat to the atmosphere, a worldwide process described in detail in a remarkable essay by Malkus (1962). But why should latent heat transfer be so efficient? Evaporative cooling could conceivably depress sea surface temperatures to the point where little heat could be transferred to the atmosphere, sensible or latent.

In most of the heat budget and heat transport studies carried out so far attention was focussed exclusively on either the atmosphere or the ocean. The above questions regarding poleward heat transport and its partitioning between

atmosphere and ocean, however, cannot be answered if one of the partners is considered in some sense inert. The few studies in which both atmosphere and ocean were taken to be active tend to be so complex as to obscure the important physical controls (e.g. the numerical model studies of the interacting atmospheric and oceanic boundary layers by Pandolfo and his associates, Pandolfo and Jacobs, 1972; Brown et al. 1981). Undoubtedly, a fully realistic simulation of air-sea interaction requires this degree of complexity. However, it is likely that considerable insight can be gained from a much simpler analytical model in which some of the more complex processes are suitably parameterized. The present study is an attempt to formulate such an analytical model of the interacting tropical and subtropical atmospheric and oceanic boundary layers, explicitly taking into account advection and turbulent transfer processes only, and restricting consideration to shallow surface mixed layers.

In order to avoid explicit consideration of such complex thermodynamic processes as cloud formation, gas and cloud radiation, it is necessary to restrict the atmospheric part of the system considered to the mixed layer below cloud base. The potential temperature θ_u and specific humidity q_u "above" cloud base then become external parameters representing the end product of complex atmospheric interactions. This means that some key physical processes are at best crudely parameterized by θ_u and q_u , limiting the insight one can gain from the model. Nevertheless, the double mixed layer model yields more insight than a single layer one, and supplies some limited answers to the questions raised above.

Although mixed layer models have been widely discussed, a number of pitfalls must be avoided in their formulation. Because the literature contains many misleading or downright erroneous statements on mixed layer balances, the

problem is carefully considered in a general way before writing down the balance equations required in the argument.

Conservation laws with open boundaries

Consider the atmospheric and oceanic surface mixed layers in contact, bounded above and below by a cloud-base inversion layer and a diffusion floor, at height $z = Z(x,y,t)$ above sea level and depth $z = -h(x,y,t)$ below (Fig. 2). The equation of continuity and the conservation law for a conservative property in either layer will be written, using suffix notation on this one occasion:

$$\begin{aligned} \frac{\partial u_i}{\partial x_i} &= 0 \\ \frac{\partial \chi}{\partial t} + \frac{\partial}{\partial x_i} (u_i \chi) &= - \frac{\partial F_i}{\partial x_i} \end{aligned} \quad (1)$$

where χ is the property in question and F_i are turbulent flux components.

The inversion layer and the mixed layer floor are not fixed either in space or relative to the fluid so that Z and h are not, in general, constant, and there is, in general, a non-zero velocity of advance relative to the air or water:

$$\begin{aligned} w_a &= \frac{dZ}{dt} - w(Z) \neq 0 \\ w_w &= \frac{dh}{dt} + w(h) \neq 0 \end{aligned} \quad (2)$$

where $w(Z)$, $w(h)$ are vertical fluid velocities at the two interfaces.

It is customary to refer to w_a and w_v as "entrainment" velocities in analogy with plume and jet entrainment problems. Applied to a density interface, or a separation surface defined in some other way, the term is in many respects a misnomer, because it implies the kind of one-way progress associated with the growth of jets and plumes. It is more illuminating to think of such an interface as a shock-front propagating relative to the fluid in either direction, i.e. with positive or negative w_a or w_v . However, bowing to custom, the usual terminology will be retained here, and negative values of w_a and w_v will be labelled "detrainment".

Depth-integrated balance equations are used in the discussion below. Given that the upper and lower boundaries of the systems considered are "open", i.e. z and h variable, care is required in the integration of the conservation laws, observing relationships of the kind:

$$\int_0^z \frac{\partial}{\partial x} (u\chi) dz = \frac{\partial}{\partial x} \int_0^z u \chi dz - u(z)\chi(z) \frac{\partial z}{\partial x} \quad (3)$$

Writing

$$\begin{aligned} U &= \int_0^z u dz & V &= \int_0^z v dz \\ C &= \int_0^z \chi dz \end{aligned} \quad (4)$$

one readily finds

ORIGINAL PAGE IS
OF POOR QUALITY

$$\frac{\partial U}{\partial x} + \frac{\partial V}{\partial y} = u(z) \frac{\partial Z}{\partial x} + v(z) \frac{\partial Z}{\partial y} - w(z) = w_a - \frac{\partial Z}{\partial t} \quad (5)$$

where w_a is as defined in Eq.(2). The depth integrated conservation law becomes:

$$\frac{\partial C}{\partial t} + \frac{\partial}{\partial x} \left(\frac{UC}{Z} \right) + \frac{\partial}{\partial y} \left(\frac{VC}{Z} \right) = w_a \chi(z) - F_z(z) + F_z(0) + \Delta \quad (6)$$

where Δ is the divergence of "diffusive" horizontal flux (including turbulent and "shear" diffusion):

$$\Delta = - \int_0^Z \frac{\partial F_x}{\partial x} dz - \int_0^Z \frac{\partial F_y}{\partial y} dz - \int_0^Z \left(u - \frac{U}{Z} \right) \left(\chi - \frac{C}{Z} \right) dz - \int_0^Z \left(v - \frac{V}{Z} \right) \left(\chi - \frac{C}{Z} \right) dz \quad (7)$$

The evolution of the boundary layers will be supposed sufficiently slow so that Δ may be ignored. Also, the layers will be supposed well enough mixed to write with a good approximation:

$$\chi \approx \frac{C}{Z} \quad u \approx \frac{U}{Z} \quad v \approx \frac{V}{Z} \quad (8)$$

This applies below the inversion layer. Above that layer the concentration is different, $\chi = \chi_u$, say. Given this discontinuity, $\chi(z)$ in Eq.(6) is indeterminate unless one specifies the sign of w_a . For w_a positive, $\chi(z) = \chi_u$, otherwise $\chi(z) = \chi$:

$$\begin{aligned} \chi(z) &= \chi(z)_+ = \chi_u & (w_a > 0) \\ \chi(z) &= \chi(z)_- = \chi & (w_a < 0) \end{aligned} \quad (9)$$

For the case of positive w_a , Eq. (6) now reduces to

$$z \frac{d\chi}{dt} = w_a (\chi_u - \chi) - F_z(z) + F_z(0) \quad (10)$$

where

$$\frac{d\chi}{dt} = \frac{\partial \chi}{\partial t} + u \frac{\partial \chi}{\partial x} + v \frac{\partial \chi}{\partial y}$$

and $F_z(z)$ and $F_z(0)$ are vertical turbulent fluxes across the inversion and the sea surface respectively. A similar treatment of the water side yields:

$$\begin{aligned} \frac{\partial u}{\partial x} + \frac{\partial v}{\partial y} &= w_w - \frac{\partial h}{\partial t} \\ h \frac{d\chi}{dt} &= w_w (\chi_h - \chi) - F_z(0) + F_z(-h) \end{aligned} \quad (11)$$

where χ_h is the concentration below the mixed layer floor, again for the case of $w_w > 0$. A source term is readily added to the right hand side, e.g. to represent enthalpy gain by net radiation. In the case of detrainment, i.e. a convergent mixed layer the equations remain correct with w_a or w_w set equal to zero. Physically, the average mixed layer temperature is unaffected by a contraction of the system's boundary. It is easily possible to miss this point (Behringer and Stommel, 1981).

ORIGINAL PAGE IS
OF POOR QUALITY

Mixed layer models described in the literature are often formulated by postulating $F_z(Z)$ to be zero (e.g. Tennekes and Driedonks, 1981; Niller and Kraus, 1977). This is an approximation inappropriate in the present context. At cloud base, in the presence of penetrative convection, the turbulent flux $F_z(Z)$ often greatly exceeds the entrainment rate $w_a(\chi_u - \chi)$ (e.g. Betts, 1976).

Furthermore, in a number of publications the "entrainment flux" $w_a(\chi_u - \chi)$ has been identified with the turbulent flux $F_z(Z)$, a very confusing step after first postulating vanishing $F_z(Z)$. "Entrainment flux" arises from the choice of a system boundary moving relative to the fluid: as more extraneous fluid is incorporated within the system, the latter's average temperature, or humidity, or whatever scalar property, changes. Rapid equalization of the property within the system implies considerable turbulent flux divergences. However, this is perfectly consistent with zero flux at the chosen moving boundary: peak downward heat flux in the atmospheric mixed layer (to take a concrete example) occurs some distance below the zero flux level (see e.g. Ball, 1960). Confusing "entrainment flux" with turbulent flux makes it difficult to reconcile mixed layer or "slab" models with more realistic continuum models, a very undesirable outcome (Deardorff and Mahrt, 1982).

Turbulent fluxes

Atmospheric fluxes of interest are those of heat and water vapor. Across the air-sea interface these are described by the well-known bulk relationships (e.g. Brutsaert, 1982):

$$F_{Hz}(0) \equiv \frac{H_s(0)}{\rho_a c_{pa}} = c_H u_* (\theta - \theta_a)$$

ORIGINAL PAGE IS
OF POOR QUALITY

(12)

$$F_{qz}(0) = c_q u_* (q_s - q)$$

where H_s is sensible heat flux in $W m^{-2}$, F_{Hz} the same in "kinematic" units, u_* is friction velocity, q_s saturation specific humidity at the sea surface temperature, c_H Stanton number, and c_q Dalton number. Over a small range of temperature the saturation specific humidity-temperature relationship may be linearized:

$$q_s = q_{s0} + \gamma \theta \quad (13)$$

where θ is sea surface temperature excess over some specific reference temperature. For 25°C as reference, $q_{s0} = 0.02$ (kg vapor per kg moist air) and $\gamma = 1.20 \times 10^{-3} K^{-1}$. The atmospheric mixed layer temperature θ_a is to be understood as potential temperature.

The turbulent flux of heat and vapor across the inversion layer at cloud base can be similarly parameterized (Betts, 1976):

$$\frac{H_i(z)}{\rho_a c_{pa}} = w_* (\theta_a - \theta_u) \quad (14)$$

$$F_{qz}(z) = w_* (q - q_u)$$

where θ_u , q_u are potential temperature and specific humidity above the inversion and w_* is a mass transfer velocity associated with the "venting"

of the boundary layer by penetrative convection. This process brings about an exchange of air across the interface in addition to any entrainment, i.e. it transfers heat and moisture even when there is no entrainment, $dZ/dt - w(Z) = 0$. As pointed out earlier, in mixed layer models this flux component is often ignored, a step certainly inadmissible at cloud base.

In the heat balance of the mixed layer in water the same heat flux $H_S(0)$ appears as on the air side, and is in kinematic units appropriate to the water side:

$$\frac{H_S(0)}{\rho_w c_w} = c_H u_* (\theta - \theta_a) \frac{\rho_a c_{pa}}{\rho_w c_w} \quad (15)$$

with ρ_w , c_w density and specific heat of seawater.

The latent heat loss associated with evaporation is:

$$\frac{H_L(0)}{\rho_w c_w} = L c_q u_* (q_s - q) \frac{\rho_a}{\rho_w c_w} \quad (16)$$

where L is latent heat of evaporation. The net heat gain of the sea surface by radiation will be designated $H_r [W m^{-2}]$.

Turbulent heat flux across the oceanic mixed layer floor is generally thought negligible, but for consistency it will be retained for now:

$$F_z(-h) = w_{**} (\theta_h - \theta) \quad (17)$$

where w_{**} is a mixed layer floor mass or heat transfer velocity and θ_h is temperature below that floor. The transfer velocity w_{**} may become significant when there is turbulence on both sides of the interface, as often happens in shallow seas.

Balance equations **ORIGINAL PAGE IS
OF POOR QUALITY**

The balance equations for enthalpy in water and in air, and for water vapor in air now become, putting θ or q for χ in Eq.(10), and substituting the various fluxes:

$$h \frac{d\theta}{dt} = (w_w + w_{**}) (\theta_h - \theta) + \frac{H_r}{\rho_w c_w} - c_H u_* (\theta - \theta_a) \frac{\rho_a c_{pa}}{\rho_w c_w} - L c_q u_* (q_s - q) \frac{\rho_a}{\rho_w c_w} \quad (18)$$

$$z \frac{d\theta_a}{dt} = (w_a + w_*) (\theta_u - \theta_a) + c_H u_* (\theta - \theta_a)$$

$$z \frac{dq}{dt} = (w_a + w_*) (q_u - q) + c_q u_* (q_s - q)$$

It is convenient to introduce the following normalized variables:

$$v_* = c_H u_* \frac{\rho_a c_{pa}}{\rho_w c_w} \quad (\text{velocity scale in water})$$

$$\alpha = \frac{w_w + w_{**}}{v_*} \quad (\text{mass transfer constant in water})$$

$$\beta = \frac{w_a + w_*}{c_H u_*} \quad (\text{mass transfer constant in air})$$

$$\mu = \frac{c_q}{c_H} = 1 \quad (\text{ratio of Dalton and Stanton numbers})$$

(19)

ORIGINAL PAGE IS
OF POOR QUALITY

$$l = \frac{L c_q \gamma}{c_{pa} c_H} \quad (\text{nondimensional latent heat})$$

$$\theta_d = \frac{q - q_{so}}{\gamma} \quad (\text{mixed layer wet bulb temperature at sea level})$$

$$\theta_{du} = \frac{q_u - q_{so}}{\gamma} \quad (\text{wet bulb temperature above cloud base, at sea level pressure})$$

$$\theta_r = \frac{H_r}{\rho_w c_w v_*} \quad (\text{temperature scale of radiant heating})$$

As indicated above, the ratio μ will be supposed unity and is not shown in the equations below. The replacement of specific humidity by wet bulb temperature implies the choice of a reference temperature, at which the saturation specific humidity is q_{so} (Eq.13). For simultaneous validity of all three Eqs. (18) it is, of course, necessary to choose the same reference temperature and consider θ , etc. departures from the reference state.

In considering steady state balance or short term, local changes it is convenient to suppose the air temperature above cloud base constant and choose it for the reference temperature. The equations simplify somewhat by writing in such cases:

$$\theta_u = 0$$

(20)

$$q_{so} \equiv q_s(\theta_u)$$

The more general formulation, with θ_u retained as a forcing variable, is required in considering seasonal and latitudinal changes.

In terms of the normalized variables Eqs.(18) become:

$$\begin{aligned} \frac{h}{v_*} \frac{d\theta}{dt} &= \alpha(\theta_h - \theta) - \theta + \theta_a - \lambda(\theta - \theta_d) + \theta_r \\ \frac{z}{c_H u_*} \frac{d\theta_a}{dt} &= \beta(\theta_u - \theta_a) + \theta - \theta_a \\ \frac{z}{c_H u_*} \frac{d\theta_d}{dt} &= \beta(\theta_{du} - \theta_d) + \theta - \theta_d \end{aligned} \quad (21)$$

These are inhomogeneous equations for water temperature θ , potential air temperature θ_a , and wet bulb temperature θ_d . The forcing terms are the radiant heating temperature scale θ_r , potential temperature θ_u and wet bulb temperature θ_{du} above cloud base, as well as water temperature θ_h below the mixed layer. With the coefficients supposed independent of θ , θ_a and θ_d the equations are linear. However, at least the mass transfer constant β is a function of buoyancy flux, i.e. of the air-sea temperature difference $\theta_a - \theta$ and of the humidity θ_d . In the following, the problem is discussed first for fixed β . Later, the dependence of β on buoyancy flux is considered. Other coefficients in (21) will be supposed constant.

Steady state solution

One would expect a time-independent solution of Eqs.(21) to model annual average conditions. Such a solution is readily found after setting the left-hand side of the three equations zero:

ORIGINAL PAGE IS
OF POOR QUALITY

$$\theta = \frac{(1 + \beta) (\alpha \theta_h + \theta_r) + \beta \theta_u + \beta l \theta_{du}}{\alpha(1 + \beta) + \beta(1 + l)}$$

$$\theta_a = \frac{\theta + \beta \theta_u}{1 + \beta} \quad (22)$$

$$\theta_d = \frac{\theta + \beta \theta_{du}}{1 + \beta}$$

Key parameters in these expressions are the two nondimensional mass transfer constants α and β . A significant result follows at once from the definition of α and typical characteristics of subtropical and tropical mixed layers, listed here in Table 1. The scale velocity in water, v_* , is of order $0.3 \times 10^{-5} \text{ m s}^{-1}$. At the mixed layer floor, the mass transfer velocity w_{**} , which parameterizes turbulent flux, is certainly much smaller than v_* . The entrainment velocity w_w is comparable to v_* only in regions of intense upwelling, primarily near the equator. Wyrtki (1981) estimates w_w to be 10^{-5} m s^{-1} at the equator, corresponding to $\alpha = 3$. Similar upward velocities are found in narrow coastal upwelling regions (Mooers et al. 1976). However, over the subtropical anticyclonic oceanic gyres the surface layer is convergent, so that there is detrainment and $w_w = 0$ applies in Eqs.(18), at least on an annual average. Thus over most of the tropical and subtropical ocean $\alpha \ll 1$. In these locations terms multiplied by α may be dropped from Eqs.(22).

With the choice of reference state above cloud base (Eq.20), and $\alpha = 0$, the following expression is obtained for sea surface temperature:

$$\frac{(1 + l)\theta}{\theta_r} = \beta^{-1} + 1 + \frac{l\theta_{du}}{\theta_r} \quad (23)$$

$$(\alpha \approx 0)$$

This now contains only three nondimensional parameters. One of them, $\Delta\theta_{du}/\theta_r$, is a ratio of two forcing terms, representing respectively the temperature depressing effect of evaporation (note that with the choice of reference state according to Eq. (20) θ_{du} is negative) and radiant heating. As shown in Table 1, typical values are $\Delta\theta_{du} \approx -17$ K and $\theta_r = 15$ K, giving a ratio somewhat greater than one, with a negative sign. The sea surface temperature is generally within 1 or 2 K of the temperature above cloud base. This implies that β cannot be small compared to unity, i.e. that $w_a + w_s$ has to be of order $c_H u_s$. Physically, the heat transfer across the cloud base inversion has to be about as efficient as across the sea surface, if measured by the respective heat transfer velocities.

The effective heat transfer velocity $w_a + w_s$ was earlier seen to consist of the inversion layer velocity dZ/dt , the subsidence velocity $-w$, and the velocity w_s parameterizing turbulent exchange. Of these, the first two can be readily estimated from data summarized by Malkus (1962): dZ/dt no more than about $6 \times 10^{-4} \text{ m s}^{-1}$, $-w$ about $3 \times 10^{-4} \text{ m s}^{-1}$, or a total entrainment velocity w_a of about 10^{-3} m s^{-1} . The sea surface heat transfer velocity $c_H u_s$ is, on the other hand, typically 10^{-2} m s^{-1} . It follows that the mass transfer velocity parameterizing turbulent flux at cloud base, w_s , has to be an order of magnitude greater than w_a .

Over the Venezuela rain forest, a careful analysis of observations by Betts (1976) yielded a mass transfer velocity w_s of 0.13 m s^{-1} . For $c_H u_s$ as listed in Table 1 this would yield $\beta = 13$ and $\theta \approx \theta_a \approx 0$, $\theta_d \approx \theta_{du}$, or mass transfer so effective as to erase any property differences across the cloud base layer. However, the buoyancy flux in that situation was considerably larger than found over the sea surface. The relationship of β to the

ORIGINAL PAGE IS
OF POOR QUALITY

Table 1

Typical parameters of trade wind region

H_r , $W m^{-2}$	180
$c_H u_*$, $m s^{-1}$	0.01
v_* , $m s^{-1}$	$0.3 \cdot 10^{-5}$
θ_r , K	15
L , $J kg^{-1}$	$2.44 \cdot 10^6$
c_{pa} , $J kg^{-1} K^{-1}$	1030
γ , K^{-1}	$1.2 \cdot 10^{-3}$
l	2.78
θ_{du} , K	- 6

buoyancy flux over the ocean is discussed in greater detail below; here the tentative conclusion is that β is of order unity.

Consider next regions of intense upwelling where α is of order unity. The first of Eqs. (22) may be rewritten as:

$$\theta - \theta_h = \frac{\theta_r + \beta(1 + \beta)^{-1} \theta_{du} - \beta(1 + \beta)^{-1} (1 + \ell) \theta_h}{\alpha + \beta(1 + \beta)^{-1} (1 + \ell)} \quad (24)$$

This gives directly the temperature elevation of the mixed layer over deeper water. The three terms in the numerator are all of the same order, the middle one negative. With the typical parameters of Table 1 and $\alpha = 3$, $\beta = 1$, $\theta_h = -4$ K one finds $\theta - \theta_h$ about 3 K. The value $\theta - \theta_h = 3$ K is exactly what was taken to be the mixed layer temperature elevation by Wyrski (1981) in his analysis of the equatorial oceanic heat budget.

Although the equilibrium solution does not simulate temperature and humidity relationships in the interacting mixed layers in a fully realistic manner, with $\beta = 1$ it reflects the partitioning of the radiant heat gain qualitatively correctly. With the left-hand side of the first Eq. (21) set equal to zero the only term representing oceanic heat retention is the entrainment term, $\alpha(\theta_h - \theta)$. When α is negligible, the radiant heat gain is all balanced by sensible and latent heat loss: with significant α , oceanic heat retention competes effectively for some of the heat gain. In the two typical cases discussed before the partitioning is

	Subtropical gyre $\beta = 1$ $\alpha = 0$		Equatorial upwelling region $\beta = 1$ $\alpha = 3$	
	K	%	K	%
Radiant heat gain, θ_r	15	100	15	100
Latent heat loss, $\ell(\theta - \theta_d)$	13.24	88.3	6.82	45.5
Sensible heat loss, $\theta - \theta_a$	1.76	11.7	- 0.55	- 3.7
Oceanic heat retention, $\alpha(\theta - \theta_h)$	0	0	8.72	58.2

ORIGINAL PAGE 13
OF POOR QUALITY

The major difference between the subtropical gyres and the equatorial upwelling region is that large reduction of latent heat loss and its replacement by oceanic heat retention in the divergent mixed layer as the most important balance term for the radiant heat gain. This remains basically true even when storage and advection are taken into account, see later discussion.

Adjustment to equilibrium

Whether or how closely the steady state solutions discussed above are approached in a continuously varying system depends on the rate of adjustment to equilibrium. This can be determined by finding the solutions of the homogeneous equations (21), with the forcing terms set equal to zero,

$\theta_h = \theta_r = \theta_{du} = 0$, and still with the reference temperature choice of Eq.(20):

$$\theta(1 + \alpha + \ell + \epsilon^{-1}D) - \theta_a - \ell\theta_d = 0$$

$$\theta_a(1 + \beta + D) - \theta = 0 \tag{25}$$

$$\theta_d(1 + \beta + D) - \theta = 0$$

ORIGINAL PAGE IS
OF POOR QUALITY

where

$$D = \frac{Z}{c_H u_*} \frac{d}{dt} \quad \epsilon^{-1} = \frac{h}{Z} \frac{c_H u_*}{v_*}$$

For the typical values quoted in Table 1 $\epsilon^{-1} = 278$, so that ϵ is small compared to unity. Physically, ϵ represents the ratio of the heat capacity of a unit area column of air (height Z) to that of water, depth h . The determinant of (25) must vanish for homogeneous solutions to exist:

$$(1 + \beta + D) \left[(1 + \beta + D)(1 + \alpha + l + \epsilon^{-1}D) - l - 1 \right] = 0 \quad (26)$$

One root is clearly

$$D_1 = - (1 + \beta) \quad (27)$$

Further inspection reveals that one of the remaining roots is of order unity, the other of order ϵ . To order ϵ these are:

$$D_2 = - (1 + \beta) - \epsilon \frac{1 + l}{1 + \beta} + O(\epsilon^2)$$

$$D_3 = - \epsilon (\alpha + \beta \frac{1 + l}{1 + \beta}) + O(\epsilon^2) \quad (28)$$

ORIGINAL PAGE IS
OF POOR QUALITY

Suppose now that the system starts from some arbitrary non-equilibrium state at time $t = 0$, given by initial temperatures θ_o , θ_{ao} and θ_{do} . Temperature and humidity changes in the course of adjustment to equilibrium are then given by

$$\begin{aligned}\theta'_j &= \theta_j - \bar{\theta}_j = A_{ji} \exp(-k_i t) \\ C_j &\equiv \theta_{jo} - \bar{\theta}_j = \sum_i A_{ji} \\ -k_i &= \frac{C_H u_*}{Z} D_i\end{aligned}\tag{29}$$

where an overbar designates the previously found steady state solution, j is successively no subscript (water), subscript a or d , and $i = 1, 2, 3$, with summation over i implied. After some routine calculations one finds the temperature perturbations θ'_j expressed in terms of their initial values C_j , to zeroth order in ϵ :

$$\begin{aligned}\theta'_a &= l \frac{C_a - C_d}{1 + l} e^{-k_1 t} + \left[\frac{C_a}{1 + l} + \frac{C_d}{1 + l} - \frac{C}{1 + \beta} \right] e^{-k_2 t} \\ &\quad + \frac{C}{1 + \beta} e^{-k_3 t} \\ \theta'_d &= \frac{C_d - C_a}{1 + l} e^{-k_1 t} + \left[\frac{C_a}{1 + l} + \frac{C_d}{1 + l} - \frac{C}{1 + \beta} \right] e^{-k_2 t} \\ &\quad + \frac{C}{1 + \beta} e^{-k_3 t} \\ \theta' &= C e^{-k_3 t}\end{aligned}\tag{30}$$

ORIGINAL PAGE IS
OF POOR QUALITY

The sea surface temperature simply adjusts to its equilibrium value on the slow time scale k_3^{-1} . The air temperature and specific humidity initially also change on the fast time scales k_1^{-1} and k_2^{-1} , but at $t \gg k_1^{-1}$ they just follow the sea temperature. For $\alpha = 0$, $\beta = 1$ and data in Table 1 the value of k_3^{-1} is 0.88×10^7 s, or 102 days. The time scales k_1^{-1} and k_2^{-2} are the same to zeroth order in ϵ and do not depend on α . For $\beta = 1$ and data of Table 1 their typical value is $k_1^{-1} = 3 \times 10^4$ s or 8.3 hrs. Physically, changes on time scale k_1^{-1} represent the adjustment of the specific humidity in the atmospheric mixed layer, those on scale k_2^{-1} of the air temperature, while the process on time scale k_3^{-1} is clearly the adjustment of the heat content of the oceanic mixed layer.

The above calculations have revealed the time scales of adjustment, but are realistic models only at a coastline (e.g. the African coast of the North Atlantic) where the air blowing from land adjusts to the balances dictated by the oceanic mixed layer. In mid-oceanic regions local changes ($\partial/\partial t$) arise in response to diurnal and seasonal variations of radiant heating, as well as of the atmospheric temperature and humidity above cloud base. These may be modeled by harmonic forcing terms. Advective changes result from the global scale gradients of the forcing terms, coupled with along-gradient flow. The time dependent response to general, variable forcing is also readily written down and serves as a basis for considering local effects of cold air and water advection. These effects are discussed in the next two sections.

ORIGINAL PAGE IS
OF POOR QUALITY

Response to periodic forcing

The typical time scales k_1^{-1} and k_3^{-1} are fortuitously close to the two principal frequencies of radiant heating, the diurnal and the annual:

$$\omega_D = \frac{2\pi}{\text{day}} = 0.73 \times 10^{-4} \text{ s}^{-1}$$

$$\omega_A = \frac{2\pi}{\text{year}} = 2 \times 10^{-7} \text{ s}^{-1}$$

To consider the response to periodic forcing at these frequencies let the radiant heat gain be written

$$\theta_r = \bar{\theta}_r + \theta_r' e^{i\omega t} \quad (31)$$

It is only necessary to calculate the response to the periodic part, setting at first $\theta_{du} = \theta_h = \bar{\theta}_r = 0$ in Eq.(21), retaining for now the reference temperature choice of Eq.(20) and supposing θ , θ_a and θ_d to vary periodically:

$$\theta = \theta' e^{i\omega t} \quad \theta_a = \theta_a' e^{i\omega t} \quad \theta_d = \theta_d' e^{i\omega t} \quad (32)$$

where the amplitudes θ' , etc. may be complex. Equations (21) reduce to:

$$\theta_a' (1 + \beta + i\sigma) = \theta'$$

$$\theta_d' (1 + \beta + i\sigma) = \theta' \quad (33)$$

$$\theta' (1 + \alpha + l + \epsilon^{-1} i\sigma) = \theta_a' + l\theta_d' + \theta_r'$$

ORIGINAL PAGE IS
OF POOR QUALITY

where
$$\sigma = \frac{\omega Z}{c_H u_*} \quad (34)$$

is the nondimensional value of the forcing frequency. The solution is

$$\theta'_a = \theta'_d = \frac{\theta'_r}{m e^{i\phi}} \quad (35)$$

$$\theta' = (1 + \beta + i\sigma) \theta'_a$$

where m, ϕ are real, defined by

$$\begin{aligned} m e^{i\phi} = & \beta(1 + \ell) + \alpha(1 + \beta) - \epsilon^{-1} \sigma^{-2} + \\ & + i\sigma[\epsilon^{-1}(1 + \beta) + 1 + \alpha + \ell] \end{aligned} \quad (36)$$

Suppose that the nondimensional frequency σ is of order unity: this is the case for diurnal forcing. The leading terms in Eq.(36) are then

$$m e^{i\phi} \approx -\epsilon^{-1} \sigma^2 + \epsilon^{-1}(1 + \beta) i\sigma \quad (37)$$

so that

$$\phi = -\tan^{-1} \left[\frac{1 + \beta}{\sigma} \right]$$

$$m = \epsilon^{-1} \sigma^2 \left[1 + \frac{(1 + \beta)^2}{\sigma^2} \right]^{1/2}$$

For the typical values of Table 1, σ_D is 4.63. With $\beta = 1$, the corresponding phase angle ϕ is -23.4° , and according to Eq.(35), θ'_a and θ'_d

ORIGINAL PAGE IS
OF POOR QUALITY

lead θ'_r . However, the response is of negligible amplitude, proportional to m^{-1} , which is typically of order 10^{-4} .

In the case of seasonal heating (σ of order ϵ) it is not realistic to suppose $\theta'_u = \text{constant}$: air temperature also varies significantly above the inversion, in phase with θ'_r . Thus although $\bar{\theta}_u = 0$ may still be chosen for a reference temperature, θ'_u must be supposed variable, and so must θ'_{du} . A more complete version of Eqs.(33) is, neglecting now quantities of order σ :

$$\theta'_a (1 + \beta) = \theta' + \beta \theta'_u$$

$$\theta'_d (1 + \beta) = \theta' + \beta \theta'_{du} \quad (3E)$$

$$\theta' (1 + \alpha + \lambda + \epsilon^{-1} i\sigma) - \theta'_a - \lambda \theta'_d = \theta'_r$$

Under this set of idealizations the sea surface temperature is found to be

$$\theta' = \frac{1}{m e^{i\phi}} \left[(1 + \beta) \theta'_r + \beta \theta'_u + \beta \lambda \theta'_{du} \right] \quad (3F)$$

with

$$m e^{i\phi} = \beta(1 + \lambda) + \alpha(1 + \beta) + i\sigma \epsilon^{-1} (1 + \beta)$$

$$\text{or } \phi = \tan^{-1} \left[\frac{\epsilon^{-1} \sigma (1 + \beta)}{\beta(1 + \lambda) + \alpha(1 + \beta)} \right]$$

$$m^2 = \epsilon^{-2} \sigma^2 (1 + \beta)^2 + [\beta(1 + \lambda) + \alpha(1 + \beta)]^2$$

ORIGINAL PAGE IS
OF POOR QUALITY

For annual forcing $\sigma = \sigma_A = 0.012$, and the above relationships give for the physical parameters in Table 1, with $\alpha = 0$, $\beta = 1$:

$$\phi = 60^\circ$$

$$m = 7.67$$

The typical amplitude of the annual forcing is 75 W m^{-2} , corresponding to $\theta'_r = 6.25 \text{ K}$, while θ'_u is of order 2 K , θ'_{du} the same. The response amplitude θ' is then for $\beta = 1$ 2.7 K , lagging behind the forcing by 60° or two months. The first two of Eqs.(38) yield $\theta' = \theta'_a = 2.35 \text{ K}$, both in phase with the sea surface temperature.

A quantity of some practical interest is the seasonal heat storage in the oceanic mixed layer, represented in Eq.(21) by the term

$$S = \frac{h}{v_*} \frac{\partial \theta}{\partial t} \quad (40)$$

In the above periodic solution this varies as $i\theta'$, i.e. it leads the forcing by $(\pi/2 - \phi)$, or typically 30° , corresponding to a month. Furthermore, at this (annual) frequency the storage term is only of order unity in the first of Eqs.(21), i.e. in the heat balance of the oceanic mixed layer, not in the heat or vapor balance of the atmospheric layer. With the typical amplitudes used above, the storage term amplitude $\epsilon^{-1} \sigma \theta'$ corresponds to a dimensional value of about 90 W m^{-2} . The seasonal cycle of temperature changes and heat storage is clearly of significant amplitude.

Cold water and air advection

Advective changes may be treated much as local ones, by supposing that the forcing terms θ_u , θ_{du} and θ_r are functions of location, and replacing time by space derivations:

$$D = \frac{Z}{c_H u_*} \frac{d}{dt} \equiv \frac{ZV}{c_H u_*} \frac{d}{dy} \equiv \frac{d}{dY}$$

$$\kappa D = \frac{h}{v_*} \frac{d}{dt} \equiv \frac{hv}{v_*} \frac{d}{dy} \equiv \kappa \frac{d}{dY} \quad (41)$$

$$\kappa = \frac{hv c_H u_*}{Z V v_*} \quad Y = \frac{c_H u_* y}{Z V}$$

Here the gradients have for simplicity been supposed to point along the y axis, which is the direction of positive advection velocities V and v, in air and water respectively. The forcing terms in Eqs. (21) θ_r , θ_u and θ_{du} will all be supposed functions of the coordinate y alone:

$$\theta(1 + l + \kappa D) - \theta_a - l\theta_d = \theta_r(y)$$

$$\theta_a(1 + \beta + D) - \theta = \beta \theta_u(y) \quad (42)$$

$$\theta_d(1 + \beta + D) - \theta = \beta \theta_{du}(y)$$

$$(\alpha \approx 0)$$

The case of negligible upwelling ($\alpha = 0$) has been assumed for simplicity, because later discussion of advection will deal mainly with the subtropical gyres. The typical value of the parameter $\kappa \equiv (v/V)\epsilon^{-1}$ is now not large, but of order unity, on account of the small typical value of the advection ratio v/V . Usual advection velocities are $v = 0.05 \text{ m s}^{-1}$ and

ORIGINAL PAGE IS
OF POOR QUALITY

$V = 5 \text{ m s}^{-1}$, giving $\kappa = 2.78$. The nondimensional distance Y is scaled by $ZV/c_H u_*$, which is typically 300 km.

Upon eliminating θ_a and θ_d from Eqs. (42) one finds the single equation for sea surface temperature:

$$\kappa D^2 \theta + [1 + l + \kappa(1 + \beta)] D \theta + \beta(1 + l) \theta = \phi(Y) \quad (43)$$

where $\phi(Y)$ is the effective forcing function for sea surface temperature:

$$\phi(Y) = (1 + \beta + D) \theta_r + \beta \theta_u + \beta l \theta_{du}$$

The characteristic equation derived from (43) has roots r_1 , r_2 , given by

$$r_1 + r_2 = - \left[\frac{1 + l}{\kappa} + 1 + \beta \right] \quad (44)$$

$$r_1 r_2 = \frac{(1 + l)}{\kappa}$$

The solution of (43) is:

$$\theta = \frac{1}{\kappa(r_2 - r_1)} \int_0^\infty \left(e^{-r_1 \eta} - e^{-r_2 \eta} \right) \phi(Y - \eta) d\eta \quad (45)$$

The result shows that the forcing terms over a "backward" ($Y' < Y$) sector of the y axis, from where the advection comes, influence the local temperature. With r_1 , r_2 of order unity, the width of the influence zone is the scale of the Y variable, earlier seen to be typically 300 km. This is small on a global scale and it is therefore realistic to replace the forcing function $\phi(Y)$ by its linear expansion:

ORIGINAL PAGE IS
OF POOR QUALITY

$$\phi(Y - \eta) = \phi(Y) - \eta \frac{d\phi}{dY} \quad (46)$$

Substitution into (45) then yields:

$$\begin{aligned} \theta &= \frac{\phi(Y)}{\kappa r_1 r_2} - \frac{r_1 + r_2}{\kappa r_1^2 r_2^2} \frac{d\phi}{dY} = \\ &= \frac{(1 + \beta) \theta_r + \beta \theta_u + \beta l \theta_{du}}{\beta(1 + l)} + \frac{1}{\beta(1 + l)} \frac{d\theta_r}{dY} \\ &- \left[\frac{1}{\beta} + \kappa \frac{1 + \beta}{\beta(1 + l)} \right] \frac{d\phi}{dY} \end{aligned} \quad (47)$$

The first term on the right is exactly the equilibrium solution $\bar{\theta}$ (Eq.22) for $\alpha = 0$. The second and third terms represent a temperature perturbation associated with cold water and air advection, which arises when the forcing functions vary in the direction of advection.

Further calculations using Eqs.(42) yield for the dry and wet bulb temperatures:

$$\theta_a + l \theta_d = \frac{1}{\kappa(r_2 - r_1)} \int_0^\infty \left(e^{-r_1 \eta} - e^{-r_2 \eta} \right) \psi(Y - \eta) d\eta \quad (48)$$

where $\psi(Y) = (1 + l) \theta_r + \beta(1 + l + \kappa D) (\theta_u + l \theta_{du})$

$$\theta_a - \theta_d = \beta \int_0^\infty \left[\theta_u(Y - \eta) - \theta_{du}(Y - \eta) \right] e^{-(1 + \beta)\eta} d\eta$$

or, using a linear expansion again, on the model of Eq.(46):

$$\theta_a + l \theta_d = \frac{\psi}{\beta(1+l)} - \left[\frac{1}{\beta} + \kappa \frac{1+\beta}{\beta(1+l)} \right] \frac{d\psi}{dy} \quad (49)$$

$$\theta_a - \theta_d = \frac{\beta}{1+\beta} (\theta_u - \theta_{du}) - \frac{\beta}{(1+\beta)^2} \left(\frac{d\theta_u}{dy} - \frac{d\theta_{du}}{dy} \right)$$

It is readily verified that the last expressions also consist of the equilibrium solution plus terms proportional to the gradients of the forcing functions. In case the latter are not known very well, the perturbations can also be expressed directly from Eqs.(42), in terms of the gradients of the dependent variables themselves:

$$\begin{aligned} \theta &= \bar{\theta} - \theta' \\ \theta_a &= \bar{\theta}_a - \frac{D\theta_a + \theta'}{1+\beta} \\ \theta_d &= \bar{\theta}_d - \frac{D\theta_d + \theta'}{1+\beta} \end{aligned} \quad (50)$$

where θ' is the sea surface temperature depression:

$$\theta' = \frac{\kappa(1+\beta) D\theta + D\theta_a + l D\theta_d}{\beta(1+l)}$$

While the gradients of the forcing terms are hard to estimate, there is good evidence on the variation of sea surface temperature in the direction of the likely surface advection over at least part of the North

Atlantic subtropical gyre. Over the northern half of this gyre surface drift is more or less along and "up" the surface temperature gradient. According to the charts of Böhnecke (1938) that gradient has a typical magnitude of $2\text{K}/1000\text{ km}$ ($2 \times 10^{-6} \text{ K m}^{-1}$), so that using earlier estimates

$$\frac{d\theta}{dy} = 0.6 \text{ K}$$

The air-sea temperature difference and the dry bulb—wet bulb difference do not change very much, and one may suppose in a first approximation:

$$\frac{d\theta_a}{dy} \approx \frac{d\theta_d}{dy} \approx \frac{d\theta}{dy} \quad (51)$$

The typical magnitudes of the advection terms in Eqs.(42) then become

$$\kappa D\theta = 1.67 \text{ K}$$

$$D\theta_a = D\theta_d = 0.6 \text{ K}$$

With the aid of Eqs.(50) these give the following corrections to the equilibrium temperature:

$$\theta' = -1.51 \text{ K}$$

$$\theta'_a = \theta'_d = -1.05 \text{ K}$$

showing that cold water and cold air advection tends to reduce the sea-air temperature difference, because it causes a greater temperature depression in the water than in the air.

ORIGINAL PAGE IS
OF POOR QUALITY

Radiation heat loss of the atmospheric mixed layer

One observation is difficult to reconcile with the heat balance equation for the atmospheric mixed layer as formulated so far (second of Eqs. 21 or 42). This is the fact that θ_a is almost always less than either θ or θ_u . Given efficient heat transfer across both interfaces, the right hand side of the second Eq. (21) is typically greater by 1 or 2 K than can be explained by cold air advection. One is led to consider heat loss by gas radiation H_{ar} , another potentially important forcing term in Eq. (18). In a normalized form appropriate for inclusion in the second of Eq. (21) this term is:

$$\theta_{ar} = \frac{H_{ar}}{\rho_a c_{pa} c_H u_*} \quad (52)$$

The magnitude of θ_{ar} may be estimated from data summarized by Fleagle and Businger (1963), according to which the air at low levels cools by radiation typically at the rate of 3 K per day or $d\theta/dt = 3 \times 10^{-5} \text{ K s}^{-1}$. The corresponding heat loss term in Eq. (18) would be

$$\frac{H_{ar}}{\rho_a c_{pa}} = z \frac{d\theta}{dt} = 1.8 \times 10^{-2} \text{ K m s}^{-1}$$

With $c_H u_* = 0.01 \text{ m s}^{-1}$ this gives a typical value for the normalized variable θ_{ar} of -1.8 K or more or less the magnitude required to balance the second Eq. (21).

The modification of the equilibrium solution (Eq. 22) on account of the θ_{ar} term consists of the inclusion of θ_{ar} in two of the three numerators, giving correction terms of

ORIGINAL PAGE IS
OF POOR QUALITY

$$\theta' = \frac{\theta_{ar}}{\beta(1 + \ell)}$$

(53)

$$\theta_a' = \frac{\theta_{ar}}{1 + \beta}$$

Typical values are -0.9 K for θ_a' , -0.5 K for θ' , comparable to the effect of cold water and air advection, and contributing further to the sea surface temperature depression, while also modifying the sea-air temperature difference, this time in a positive direction.

Heat and mass transfer through penetrative convection

In order to complete the analytical argument, it is necessary to consider the physical processes responsible for determining the value of the mass transfer coefficient β , and show that the order one typical values supposed above are plausible. The problem of mixed layer deepening (in the atmospheric or oceanic application) has an extensive literature (e.g. Niiler and Kraus, 1977; Tennekes and Driedonks, 1981) but it is almost exclusively aimed at density interfaces across which the turbulent flux is negligible, and entrainment is the only mechanism of heat and mass transfer. As pointed out above, this is not the case at cloud base, and a different approach must be adopted.

Given the intense penetrative convection at cloud base, it is reasonable to suppose that the vertical motions that "vent" the mixed layer have the velocity scale of free convection (Deardorff, 1974):

$$w_c = (BZ)^{1/3} \quad (54)$$

where B is the sea surface buoyancy flux, due to the transfer of sensible

ORIGINAL PAGE IS
OF POOR QUALITY

heat and also of water vapor (Brutsaert, 1982):

$$B = g \left[c_H u_* \frac{\theta - \theta_a}{T} + 0.61 c_q u_* (q_s - q) \right] \quad (55)$$

with T the reference absolute temperature.

The simplest parameterization scheme for the net mass transfer coefficient at cloud base is:

$$w_a + w_* = \lambda w_c \quad (56)$$

where $\lambda = \text{constant}$. This certainly does not do full justice to the physics of penetrative convection, the net mass transfer being in addition dependent on the distance z from the lower boundary, the buoyancy saltus b at the top of the mixed layer, and possibly some other factors, i.e.:

$$\lambda = \text{func} \frac{w_c^2}{bz}, \dots \quad (57)$$

Typically, however, the cloud base inversion is weak and it is not too unreasonable to suppose that turbulent transfer processes in its neighborhood are determined by the parameters characterizing the free convection regime, a supposition that leads directly to Eq.(56). This amounts to supposing that bz/w_c^2 is suitably small in the parameter range of interest.

In the case analyzed by Betts (1976) in detail the characteristic convection velocity was $w_c = 1.85 \text{ m s}^{-1}$, while the net mass transfer coefficient was empirically determined to be $w_a + w_* = 0.13 \text{ m s}^{-1}$. This gives $\lambda = 0.07$, a value that will be adopted in the following.

Combining Eqs. (54) to (56), expressing them in terms of the variables of

Eq.(19), and substituting the equilibrium relationships (22), one finds the following expression for the coefficient β (reference temperature choice according to Eq.(20):

$$\beta^2 \theta_* = \theta_a + 0.61 \gamma T \left(\theta_a - \frac{\theta_{du}}{1 + \beta} \right) \quad (58)$$

ORIGINAL PAGE IS
OF POOR QUALITY

where θ_* is a temperature scale:

$$\theta_* = \frac{c_H^2 u_*^2 T}{\lambda^3 g z} \quad (59)$$

and θ_a is given by (22).

With the above chosen value of $\lambda = 0.07$, $T = 300$ K, and the typical quantities of Table 1, one calculates

$$\theta_* = 0.167 \text{ K}$$

while $0.61 \gamma T = 0.22$. The value of β may now be determined (supposing steady state conditions) from Eq.(58) and (22), as a function of the coefficient α , and the forcing parameters θ_r , θ_{du} and θ_h .

With the typical quantities of Table 1, and for $\alpha = 0$ one finds

$$\beta = 2.3$$

Physically, such a relatively low value of β (compared to the over-land case of Betts, 1976) is due to the fact that most of the heat is transferred as latent heat, which causes only little buoyancy flux.

For $\alpha = 4.02$, β drops to zero: at this water entrainment rate, with $\theta_h = -4$ K, there is zero buoyancy flux, and by the hypothesis of Eq.(54), vanishing entrainment of air from above the atmospheric mixed layer. This asymptotic case is characterized also by

ORIGINAL PAGE IS
OF POOR QUALITY

(60)

$$\theta = \theta_a = \theta_d$$

or an atmospheric mixed layer of the same temperature as the sea surface, saturated with water vapor, clearly a somewhat unrealistic result. A value of $\beta = 1$ is reached at $\alpha = 2.57$. The precise numerical values are not significant in virtue of the uncertainty of λ , which was deduced from a single case observed over land. However, the calculations show that an order one value of β is compatible with realistically assumed properties of penetrative convection over the ocean. The value of β is kept modest, because the buoyancy flux is low at the usual relatively high rate of evaporation.

Comparison with observation

So far the emphasis in the various partial comparisons between analytical model and observation has been on the determination of the order of magnitude of the different terms in the heat and vapor balances, Eqs.(21), the transfer coefficients, cold water advection, etc. After the key parameters have been chosen, a more detailed examination of the observed temperature and humidity relationships becomes possible and should answer questions relating to warm water mass formation. Detailed relevant evidence is available in the subtropical trade wind belt, both in the form of atmospheric temperature and humidity profiles, and time histories of monthly average sea to air fluxes, air and water temperatures.

Temperature and humidity profiles in the subtropical marine boundary layer have been published by a number of investigators, including Bunker et al. (1949), taken just north of Puerto Rico in April, Fig. 3. The following

temperatures may be extracted from those data (reference $\theta_u = 0$):

$$\theta_{du} = - 11.5 \text{ K}$$

$$\theta_d = - 7.5 \text{ K}$$

$$\theta = - 1.5 \text{ K}$$

$$\theta_a = - 2 \text{ K}$$

The wind speed was about 8 m s^{-1} , from which one estimates

$$c_H u_* = 0.02 \text{ m s}^{-1}$$

The net heat gain from radiation, estimated from climatological data for this time of year at 200 W m^{-2} (Bunker, 1976), results in:

$$\theta_r = 8 \text{ K}$$

The absolute potential temperature above cloud base may be taken to have been 301 K . Substituting into Eqs.(21) one finds:

$$\frac{h}{v_*} \frac{d\theta}{dt} = - 9.2$$

$$\frac{z}{c_H u_*} \frac{d\theta_a}{dt} = 0.5 + 2\theta + \theta_{ar}$$

$$\frac{z}{c_H u_*} \frac{d\theta_d}{dt} = - 4\theta + 3.5$$

where radiation heat loss has also been explicitly included.

Allowing also for cold air advection as per earlier estimate ($D\theta = 0.3 \text{ K}$, for the high $c_H u_*$), the second and third equations come close to balance with $\beta = 0.8$. The first equation, however, shows that the water column was certainly not in thermal equilibrium: supposing the usual weak rate of cold water advection characteristic for this location, the water column was being locally cooled at a rate of some 250 W m^{-2} , while in April a heating rate of that magnitude is usual. One reason for the discrepancy is the smallness of θ_r , a direct consequence of the high wind speed, the value of $c_H u_*$ being twice the typical value listed in Table 1. Another reason is the large negative value of θ_{du} , i.e. the dryness of the air descending into the mixed layer. The example demonstrates that instantaneous or short term average temperature and flux conditions cannot be used to infer the monthly average oceanic heat retention rate. One notes also that the heat gain estimate (200 W m^{-2}) on the basis of a monthly mean may not have been appropriate.

The equilibrium sea surface temperature one calculates from (22), with allowance for cold water advection and radiation loss from the air, is $\theta = -4.3 \text{ K}$ or some 5 K lower than observed. Given an anomaly of 5 K , one expects the normalized cooling rate to be

$$\frac{h}{v_*} \frac{\partial \theta}{\partial t} = \frac{h}{v_*} k_3 \Delta \theta = 1.89 \Delta \theta = -9.5 \text{ K}$$

having used Eqs. (28) and (29). The result agrees almost exactly with the first of the balance equations (21), with observed temperatures substituted, see above. The agreement corroborates the climatologically estimated rate of cooling of 200 W m^{-2} .

ORIGINAL PAGE IS
OF POOR QUALITY

In spite of the thermal disequilibrium of the oceanic mixed layer, many aspects of the data in Fig. 3 are typical for the western North Atlantic trade wind region. The sea surface temperature is here usually slightly higher (0.5 to 1 K) than the mixed layer air temperature, but lower by about 1-2 K than the air above cloud base: there is usually a weak inversion at cloud base. The very large value of θ_{du} seems to be connected with the height of the main trade inversion. As may be seen from the figure, the local wet bulb—dry bulb temperature nearly vanishes at the top of the cloud layer. Correspondingly, the specific humidity within the cloud layer is near the saturation value at cloud top, i.e. at a height in this case of 2300 m. Cloud base is, of course, at the lifting condensation level, or where the sea level air becomes saturated. The difference in saturation specific humidities between cloud base and cloud top, and therefore θ_{du} , is a function of cloud layer depth. As Malkus (1962) discusses in detail, this depth grows from the African coast westward over the North Atlantic. The typical value of $\theta_{du} = -6$ K of Table 1 was chosen to represent an intermediate stage. Even at Puerto Rico the large wet bulb temperature depression seems excessive: $\theta_{du} = -9$ K should be more typical.

Accepting $\theta_{du} = -9 \text{ K}$ for the Puerto Rico location, using $\beta = 1$, but the more typical air-sea transfer coefficient $c_H u_* = 0.01 \text{ m s}^{-1}$ and an annual net radiation gain 180 W m^{-2} , one calculates the following equilibrium temperatures from Eq.(22):

$$\theta = 1.32 \text{ K}$$

$$\theta_a = 0.66 \text{ K}$$

$$\theta_d = -3.84 \text{ K}$$

These are clearly wrong: air below cloud base should be colder than above. Correcting for radiation loss (Eq.53) one finds the slightly more realistic results:

$$\theta = 0.84 \text{ K}$$

$$\theta_a = -0.48 \text{ K}$$

$$\theta_d = -4.08 \text{ K}$$

The calculated sea surface temperature is still much too high. However, after allowing for cold water and air advection according to Eq.(51) one arrives at:

$$\theta = -0.67 \text{ K}$$

$$\theta_a = -1.54 \text{ K}$$

$$\theta_d = -5.15 \text{ K}$$

The sea-air temperature difference is now within its typical range of $0.5 - 1.0 \text{ K}$; the dry bulb—wet bulb temperature difference is 3.6 K , which is somewhat low but not atypical, and the cloud base inversion strength is 1.54 K or pretty much as observed. Better agreement can hardly be expected.

ORIGINAL PAGE IS
OF POOR QUALITY

The main point is that without allowing for atmospheric radiation loss and cold water and air advection the long-term mean temperature-humidity relationships cannot be at all realistically simulated.

It is of interest to consider also the partitioning of the total heat gain θ_r of the oceanic mixed layer into sensible and latent heat loss and net heat retained (the latter owing to cold water advection). Assuming that the just calculated values realistically represent annual average conditions one finds the following:

	(K)	%
Heat gain, θ_r	15	100
Latent heat loss, $\ell(\theta - \theta_d)$	12.45	83
Sensible heat loss $\theta - \theta_a$.87	6
Cold water advection $vh/v_* d\theta/dy$	1.67	11

As remarked earlier, these differ little from what one deduces from the equilibrium solution. The Bowen ratio $(\theta - \theta_a)/\ell(\theta - \theta_d)$ is 7%, or a typical value. The dominance of the latent heat loss is seen to be caused by the high value of the material constant ℓ , and the high absolute value of θ_{du} (which, with β of order unity, translates into a large dry bulb—wet bulb difference in the mixed layer). As pointed out above, the high absolute value of θ_{du} derives from low saturation specific humidity at the height of the trade inversion and is, in a sense, another property of the water substance, although it is also an outcome of boundary layer processes determining the thickness of the cloud layer.

Monthly and yearly average temperatures and fluxes have also been determined from sea surface and satellite data by a number of investigators. In the North Atlantic trade wind belt a typical location is 1500 km northeast of Puerto Rico,

The partitioning of the heat gain is:

	(K)	%
net heat gain θ_r	17	100
latent heat loss $l(\theta - \theta_d)$	14	82
sensible heat loss $\theta - \theta_u$	0.5	3
cold water advection $\theta_n = v_h/v_* d\theta/dy$	2.5	15

These data are very similar to the ones just calculated from the steady state model under typical conditions. The only difference of any note is a somewhat smaller sensible heat loss, due to a small sea-air temperature difference. The correspondence establishes that the equilibrium solution of the boundary layer model, modified by an allowance for cold water and cold air advection (and with the inclusion of radiation heat loss in air) realistically simulates annual average conditions.

A perhaps more stringent test of the simple model is a comparison of results calculated for annual harmonic forcing with the observed variation of monthly mean temperatures. For this comparison it is plausible to take the value $c_H u_* = 0.008 \text{ m s}^{-1}$ deduced from the annual average temperature-flux relationships and use $\beta = 1$. The amplitude of the forcing function is $H_r' = 75 \text{ W m}^{-2}$, directly from Fig. 4. Less certain estimates are mixed layer depths of $Z = 600 \text{ m}$ and $h = 50 \text{ m}$, and seasonal fluctuation amplitudes of dry and wet bulb temperature above cloud base, $\theta_u' = \theta_{du}' = 2 \text{ K}$. The non-dimensional annual frequency is with the above value of $c_H u_*$ equal to $\sigma = 0.015$. From Eq. (39) one finds:

$$\phi = 65.62$$

$$m = 9.16$$

$$\phi' = 2.46 \text{ K}$$

$$e^{-1} \sigma \theta' = 10.27 \text{ K}$$

PRECEDING PAGE BLANK NOT FILMED

~~ORIGINAL PAGE IS
OF POOR QUALITY~~

This represents a phase lag of a little over two months, a sea surface temperature response amplitude of 2.5 K and a heat storage amplitude of 100 W m^{-2} . The latter is to be compared with the amplitude of oceanic heat retention, H_n in Fig. 4. The storage should lead the heating rate by about one month. The model predictions are very close to the observed results, considering the crudeness of some of the estimates that went into the calculations. All of the evidence confirms that $\beta = 1$ is a reasonable estimate of the cloud base mass transfer coefficient. The order of magnitude of this constant may therefore be taken as firmly established.

Modes of oceanic heat retention

What does the above analysis imply about warm water mass formation? The process takes place when and where the ocean retains a portion of its radiant heat gain, i.e. when there is net heat retention H_n on top of what is transferred to the atmospheric mixed layer:

$$H_n = H_r - c_H u_* \rho_a c_{pa} (\theta - \theta_a) - L c_q u_* \rho_a (q_s - q) \quad (61)$$

According to Eq.(18) the net heat retention is also

$$\frac{H_n}{\rho_w c_w} = h \frac{\partial \theta}{\partial t} + \underline{u} \cdot \nabla_1 \theta + (w_w + w_{**}) (\theta - \theta_h) \quad (62)$$

The right hand side of this equation shows that heat retention by the oceanic mixed layer may manifest itself in three different ways: (1) as local heating, i.e. storage, $h \partial \theta / \partial t$; (2) as horizontal cold water advection, or heating the fluid as it moves along, $\underline{u} \cdot \nabla_1 \theta$; (3) as vertical

advection, i.e. heating of fluid entrained from below, accommodated in the divergent surface layer. In the previous section storage and cold water advection were considered in detail in the North Atlantic subtropical gyre.

Fig. 4 shows net annual heat retention of order 30 W m^{-2} . According to the charts of Bunker and Worthington (1976) or of Hastenrath (1980), a similar net gain characterizes large areas of the trade wind belt, i.e. the subtropical oceanic gyres. However, these values of H_n were estimated from meteorological and satellite data as a difference between positive and negative terms in an energy budget like Eq.(18), with H_r further split into incoming and outgoing radiation. It is readily shown that the typical error of such calculations is of the same order as the calculated net heat gain, i.e. 30 W m^{-2} (Weare et al., 1981). It is therefore important to examine the oceanic evidence to see whether the net heat gain values can be substantiated.

The comparison of the boundary layer model with observation in the last section showed that the temperature-flux relationships near Puerto Rico and northwestward can only be understood if cold water advection is taken into account, at about the rate corresponding to the meteorological evidence. This rate was inferred in the section dealing with cold water advection from observed ocean surface temperature gradients and the generally accepted magnitude and direction of the surface drift over the northern portions of the subtropical gyre. Other estimates of heat gain associated with cold water advection have been made by Stommel (1979), Clarke (1979) and Behringer and Stommel (1981) at relatively low latitudes (20°N and 9°N respectively). All these estimates yielded values of order 10 W m^{-2} , in rough agreement with the charts of Bunker and Worthington for the region in question.

Another way to examine the oceanic heat retention is to calculate the global heat balance of the entire mixed layer over a subtropical gyre.

Putting $w_w + w_{**} = 0$ in Eq.(62) for the case of detrainment and dropping the storage term in a calculation of the long term mean heat gain, the equation is integrated over the area A of a gyre, enclosed by perimeter C. One finds by the divergence theorem and the water-side equivalent of Eq.(5):

$$\iint_A \frac{H}{\rho_w c_w} \frac{\partial \theta}{\partial x} dx dy = \oint_C h \theta \underline{u} \cdot \underline{n} ds - \iint_A \theta w_w dx dy \quad (63)$$

The second term on the right arises from the horizontal divergence of the flow, Eq.(5), an integral of which, adapted to the water side yields:

$$\oint_C h \underline{u} \cdot \underline{n} ds - \iint_A w_w dx dy = 0 \quad (64)$$

In these expressions ds is a line element of the perimeter C , \underline{n} its outward unit normal. The integral balances (63) and (64) can be written down à priori.

Over the subtropical gyres w_w is negative and there is net inflow at the perimeter. Let that portion of the perimeter with inflow ($\underline{u} \cdot \underline{n} < 0$) be designated C_1 , the remainder C_2 . Inflow and outflow volumes are then

$$V_1 = - \oint_{C_1} h \underline{u} \cdot \underline{n} ds \quad V_2 = \oint_{C_2} h \underline{u} \cdot \underline{n} ds \quad (65)$$

Writing θ_1 , θ_2 and θ_w for the weighted average temperatures of mixed layer inflow, outflow and detrainment, one may then express Eq. (63) as

$$\iint_A \frac{H}{\rho_w C_w} dx dy = v_1 \left[\theta_w - \theta_1 + \frac{v_2}{v_1} (\theta_2 - \theta_1) \right] \quad (66)$$

This balance contains bulk quantities not too difficult to estimate from existing information. Near the southern boundary of the subtropical gyre temperature differences are small. It is not unreasonable to suppose that any wind drift entering from the south is detrained in the interior at about the same temperature as it entered, so that it makes little contribution to Eq. (66). Total inflow into the mixed layer at the northern perimeter (near 40°N) due to wind drift alone is of order $10^7 \text{ m}^3 \text{ s}^{-1}$. This is heated, according to Böhnecke's (1938) charts, by some 5 K before being detrained. The corresponding heat gain, distributed over an area of 2000 km x 5000 km (about the area of the gyre) amounts to 20 W m^{-2} . Additional cold water advection by southward geostrophic flow increases this estimate somewhat, as does an allowance for cold surface water entering the gyre's mixed layer from the upwelling region at the eastern boundary. Crude as the oceanographic estimate may be, it is robust in the sense that neither the total southward transport across 40°N, nor the temperature rise between (say) 40°N and 20°N, nor the total area of heat gain can be seriously in error. One can therefore accept at least the global value of the net oceanic heat gain over the North Atlantic subtropical gyre as being of order $0.3 \times 10^{15} \text{ W}$, as implied by the charts of Bunker and Worthington (1976).

In the area of equatorial upwelling an important heat retention mechanism is the warming of water entering the mixed layer from below, which is accommodated in the divergent surface layer. In Eq. (18) the corresponding heat gain was expressed as $w_w(\theta - \theta_h)$, the turbulent transfer velocity w_{**} being presumably negligible. Wyrтки (1981) has examined the available evidence and concluded that upwelling velocities at the equator are of order 10^{-5} m s^{-1} . The equilibrium solution discussed briefly above with $\alpha = 3$, $\beta = 1$ corresponds roughly to this case and results in $|\theta_h - \theta| = 3 \text{ K}$, exactly the value used by Wyrтки in calculating the net horizontal heat transport away from the equatorial "cool tongue". It should be pointed out, however, that horizontal cold water advection is also important at the equator (as noted by Wyrтки), contrary to the assumptions of the simple equilibrium model.

The global heat balance for an area A of the cool tongue is, retaining the entrainment term in Eq. (62) with definitions of V_1 and V_2 as before,

$$\begin{aligned} \iint_A \frac{H_n}{\rho_w c_w} dx dy &= \oint_C h \theta \underline{u} \cdot \underline{n} ds - \iint_A w_w \theta_h dx dy \\ &= V_2(\theta_2 - \theta_h) - V_1(\theta_1 - \theta_h) \end{aligned} \quad (67)$$

According to the estimates of Wyrтки (1981), the total volume transport V_2 transporting away much of the retained heat in the surface layer is of order $50 \times 10^6 \text{ m}^3 \text{ s}^{-1}$ over a 10,000 km long piece of the cool tongue in the equatorial Pacific. The corresponding kinematic heat transport, with $(\theta_2 - \theta_h) \approx 3 \text{ K}$ is $150 \times 10^6 \text{ K m}^3 \text{ s}^{-1}$, or a large fraction of the worldwide poleward transport of heat by the ocean.

ORIGINAL PAGE IS
OF POOR QUALITY

One aspect of equatorial heat retention has been insufficiently emphasized in the literature: the $50 \times 10^6 \text{ m}^3 \text{ s}^{-1}$ of heated water moving poleward constitutes a warm water mass formed in the equatorial cool tongue. The equivalent amount of water transport moving toward the equator to supply the upwelling water has an average temperature some 3 K lower, i.e. it is a different water mass, not a recirculating one as is sometimes tacitly implied in discussions of the meridional circulation near the equator. At about 3°N and 3°S there is a total poleward moving water mass of order $M = \rho_w \times 50 \times 10^6$ and a similar equatorward moving mass, with a temperature some 3 K lower, all within 300 m or so of the surface. The poleward moving surface layer is strongly convergent beyond 3°N or 3°S because the Ekman transport drops sharply. How this warm water mass is incorporated into the equatorial near-surface circulation, and by what mechanism its replacement is supplied to the upwelling region, are two questions to which we have no answers at all at present.

Acknowledgement

The work described herein was supported by a grant from NASA entitled Warm Water Mass Formation.

References

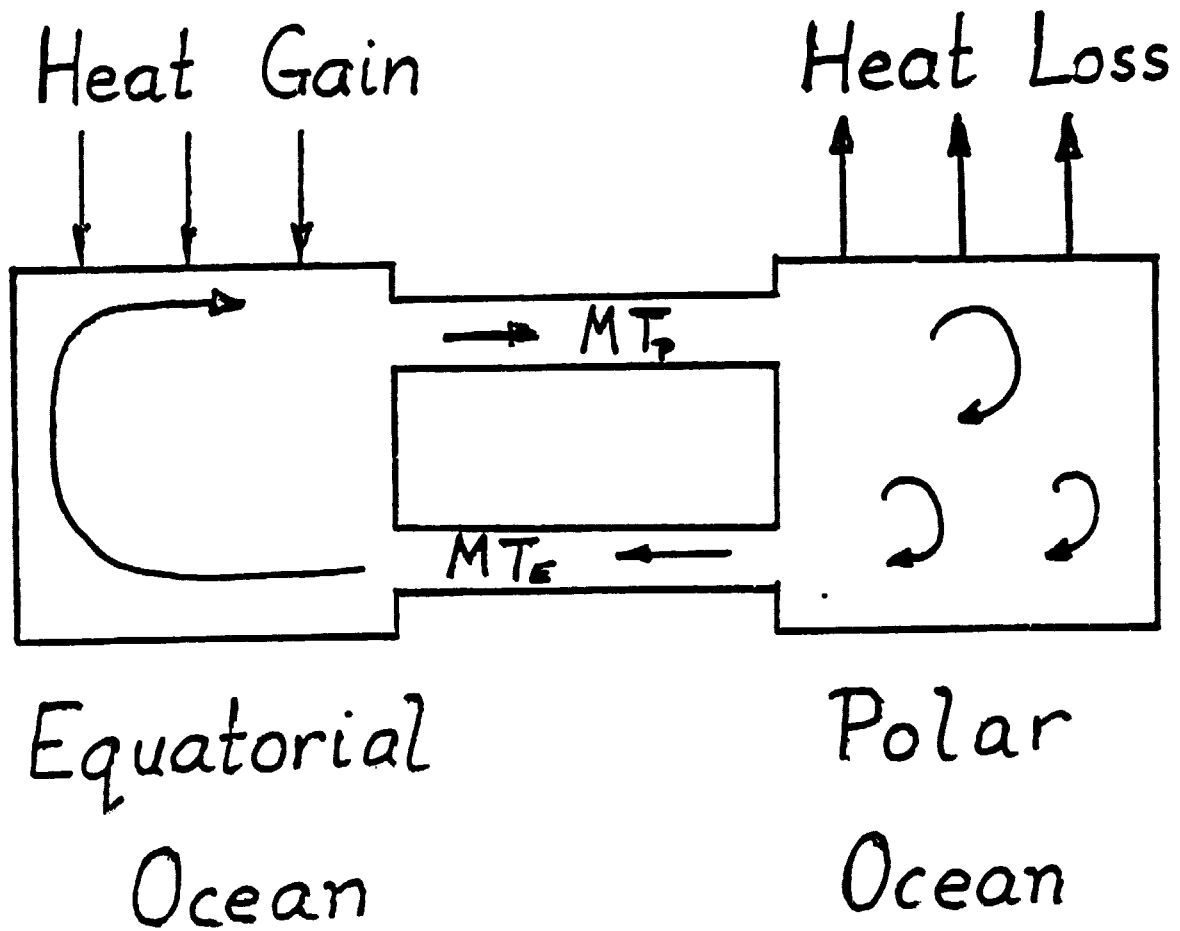
- Ball, F.K. (1960) Control of inversion height by surface heating/
Quart. J. Roy. Meteor. Soc. 85, 483-494.
- Behringer, D.W. and H. Stommel (1981) Annual heat gain in the tropical Atlantic
 computed from subsurface ocean data. J. Phys. Oceanogr. 11, 1393-1398.
- Betts, A.K. (1976) Modeling subcloud layer structure and interaction with a
 shallow cumulus layer. J. Atmos. Sci. 33, 2363-2382.
- Böhnecke, G. (1938) Temperatur, Salzgehalt und Dichte an der Oberfläche des
 Atlantischen Ozeans. English translation, Directorate of Weather,
 U.S. Army Air Forces (1943), 51 pp.
- Brown, P.S., J.P. Pandolfo and S.J. Thoren (1982) GATE Air-Sea Interaction
 I: Numerical model calculation of local sea surface temperatures on
 diurnal time scales using the GATE version III gridded global data set.
J. Phys. Oceanogr. 12, 483-494.
- Brutsaert, W.H. (1982) Evaporation into the Atmosphere. D. Reidel Publishing Co.,
 299 pp.
- Bryden, H.L. and M.M. Hall (1980) Heat transport by currents across 25° latitude
 in the Atlantic Ocean. Science 207, 884-886.
- Bunker, A.F. (1976) Computations of surface energy flux and annual air-sea
 interaction cycles of the North Atlantic Ocean. Monthly Weather Review
104, 1122-1139.
- Bunker, A.F., B. Haurwitz, J.S. Malkus and H. Stommel (1949) Vertical distribution
 of temperature and humidity over the Caribbean Sea. P.P.O.M. MIT-Woods Hole
11, 82 pp.
- Bunker, A.F. and L.V. Worthington (1976) Energy exchange charts of the North
 Atlantic Ocean. Bull. Am. Meteor. Soc. 57, 670-678.
- Clarke, R.A. (1979) Changes in the upper ocean within the C-Scale array during
 Phase III. Deep-Sea Res. GATE Supplement Vol.1, 65-127.

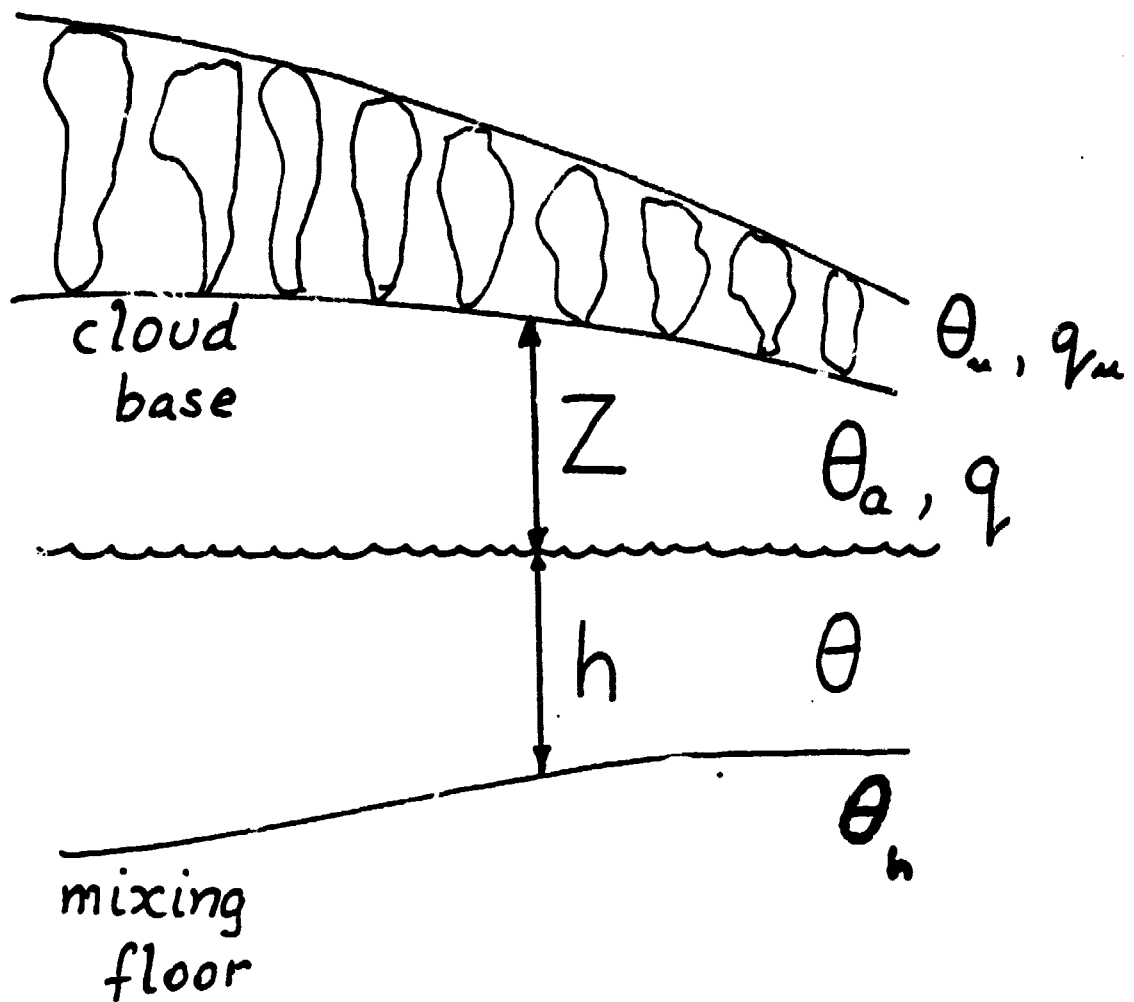
- Deardorff, J.W. (1974) Three-dimensional numerical study of the height and mean structure of a heated planetary boundary layer. Boundary Layer Meteor. 7, 81-106.
- Deardorff, J.W. and L. Mahrt (1982) On the dichotomy in theoretical treatments of the atmospheric boundary layer. J. Atmos. Sci. 39, 2096-2098.
- Hastenrath, S. (1980) Heat budget of tropical ocean and atmosphere. J. Phys. Oceanogr. 10, 159-170.
- Hastenrath, S. (1982) On meridional heat transports in the world ocean. J. Phys. Oceanogr. 12, 922-927.
- Malkus, J.S. (1962) Large scale interactions. The Sea, Vol. 1, pp. 88-294, Interscience Publishers.
- Moore, C.N.K., C.A. Collins and R.L. Smith (1976) The dynamic structure of the frontal zone in the coastal upwelling region off Oregon. J. Phys. Oceanogr. 6, 3-21.
- Nilner, P.P. and E.B. Kraus (1977) One-dimensional models of the upper ocean. Modelling and prediction of the upper layers of the ocean. Ed. E.B. Kraus, pp. 143-172. Pergamon Press, Oxford.
- Pandolfo, J.P. and C.A. Jacobs (1972) Numerical simulations of the tropical air-sea planetary boundary layer. Boundary Layer Meteor. 3, 15-46.
- Stommel, H. (1979) On the determination of water mass properties of water pumped down from the Ekman layer to the geostrophic flow below. Proc. Nat. Acad. Sci. USA 76, 3051-3055.
- Tennekes, H. and A.G.M. Driedonks (1981) Basic entrainment equations for the atmospheric boundary layer. Boundary Layer Meteor. 20, 515-531.
- Weare, B.C., P.T. Strub and M.D. Samuel (1981) Annual mean surface heat fluxes in the tropical Pacific Ocean. J. Phys. Oceanogr. 11, 705-717.
- Wyrtki, K. (1965) The average annual heat balance of the North Pacific Ocean and its relation to ocean circulation. J. Geophys. Res. 70, 4567-4559.
- Wyrtki, K. (1981) An estimate of equatorial upwelling in the Pacific. J. Phys. Oceanogr. 11, 1205-1214.

Figure Legends

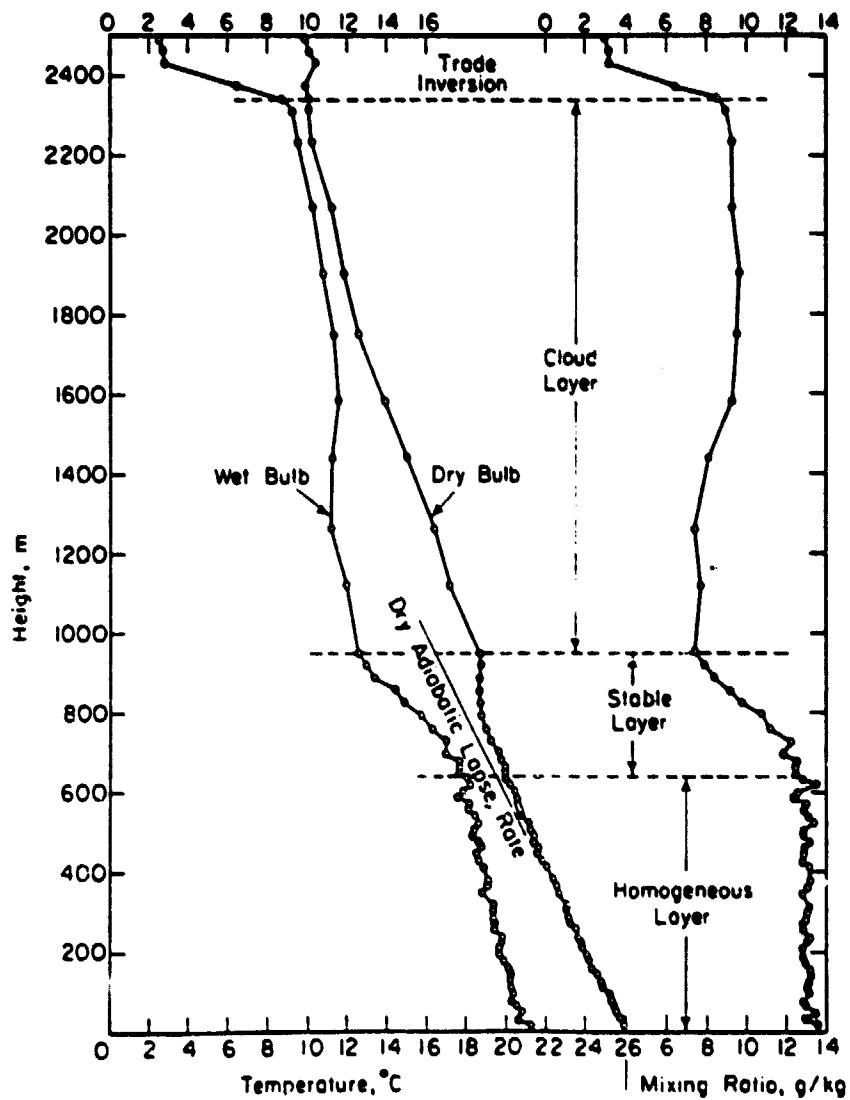
- Fig. 1 Schema of global oceanic heat transports, "cold" and "warm" water mass formation in the polar and equatorial oceans
- Fig. 2 Interacting atmospheric and oceanic mixed layers and variables of interest in the thermodynamic model
- Fig. 3 Typical profiles of temperature and humidity in the atmospheric mixed layer and above, from Bunker et al. (1949). Wind speed was 7.5 m s^{-1} , sea minus air temperature difference 0.5 K
- Fig. 4 Annual cycle of surface heat fluxes and temperatures:
 H_r net radiant heat gain by the ocean, H_s sensible,
 H_L latent heat transfer to the air, $H_n = H_r - H_s - H_L$
net oceanic heat retention, t_s sea surface, t_a air, dry bulb, t_d wet bulb temperature. From Bunker (1976), based on more than 12,000 observations in the trade wind region ($23^\circ\text{N } 52^\circ\text{W}$)

ORIGINAL PAGE IS
OF POOR QUALITY





ORIGINAL PAGE IS
OF POOR QUALITY



ORIGINAL PAGE IS
OF POOR QUALITY

